

Short-Armature Self-Excitation Type Linear Synchronous Motor for Transport System

Tsuyoshi Higuchi, Takashi Abe, Jun Oyama, Takashi Yoshida, Tadashi Hirayama
 Department of Electrical and Electronic Engineering, Nagasaki University
 1-14 Bunkyo Machi, Nagasaki, 852-8521 Japan

Abstract—In the previous paper, we proposed a long-armature type novel linear synchronous motor with half-wave rectified self excitation. The field winding was short circuited with a diode and the armature winding was usual 3-phase windings. This paper presents a short-armature type novel linear synchronous motor applicable for a transport system. Compensated short pitch windings are proposed for the armature windings in order to decrease end effect.

I. INTRODUCTION

In the previous paper, we proposed a long-armature type novel linear synchronous motor (LSM) based on "half-wave rectified self excitation principle", confirmed experimentally that the novel LSM was operated smoothly according to the principle, and constructed a simulation model using a circuit simulator [1][2]. The field winding of the motor was short circuited through a diode and the armature winding was usual 3-phase windings. DC power supply for the field excitation was not necessary because the field current was induced from the armature flux.

This paper presents a short-armature type novel LSM applicable for a transport system[3]. The novel LSM has simple and robust structure and is economical as compared with permanent magnet type LSM or conventional electromagnet type LSM. As the field flux of the novel LSM is controllable with varying amplitude of the armature current, field weakening operation can be performed easily. Here, compensated short pitch windings are proposed for the armature windings in order to increase torque and decrease end effect.

II. NOVEL LSM WITH HALF-WAVE RECTIFIED SELF EXCITATION

A. Structure of the novel LSM

Fig. 1 shows a structure of the short-armature type novel LSM with the half-wave rectified self excitation. The field windings fixed on the ground are short circuited with diodes. Onboard LSM armature has usual 3-phase armature windings and is power-supplied by a PWM inverter.

B. Principle of Self Excitation and Thrust Generation

Fig. 2 shows currents, flux, and thrust waveforms of the novel LSM. The following 3-phase currents synchronized with mover position are supplied to the 3-phase armature windings;

$$\left. \begin{aligned} i_a &= A_f(t)\sin\omega t + \sqrt{2}I_f\cos\omega t \\ i_b &= A_f(t)\sin\left(\omega t - \frac{2}{3}\pi\right) + \sqrt{2}I_f\cos\left(\omega t - \frac{2}{3}\pi\right) \\ i_c &= A_f(t)\sin\left(\omega t - \frac{4}{3}\pi\right) + \sqrt{2}I_f\cos\left(\omega t - \frac{4}{3}\pi\right) \end{aligned} \right\} \quad (1)$$

where ω : synchronous angular velocity.

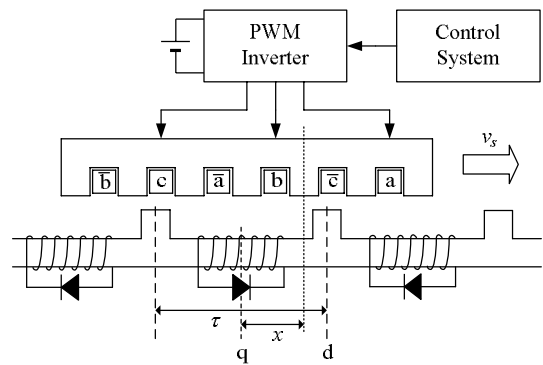


Fig. 1. Structure of the novel LSM.

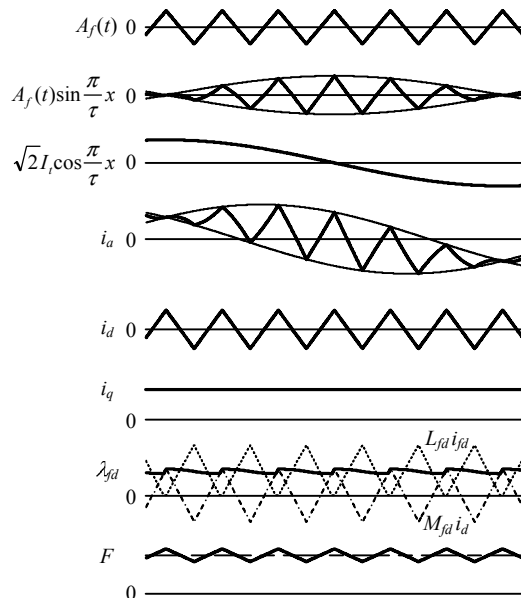


Fig. 2. Current, flux and thrust waveform.

The first term on the right-hand side of (1) is excitation current, which varies with sine of the mover position and whose amplitude is modulated by a function $A_f(t)$. Where, $A_f(t)$ is a triangular wave function with the effective value of I_f and bias frequency ω_b . The second term on the right-hand side of (1) is thrust current component.

The d-axis and q-axis currents become;

$$\left. \begin{aligned} i_d &= \sqrt{\frac{3}{2}} A_f(t) \\ i_q &= \sqrt{3} I_t \end{aligned} \right\} \quad (2)$$

Then, flux linkage $M_{fd}i_d$ is generated on the field d-axis. The field current i_{fd} is induced in the field winding to keep the maximum value of the flux. The flux linkage λ_{fd} is the sum of two flux linkages; $M_{fd}i_d$ provided by the armature excitation current and $L_{fd}i_{fd}$ by the field current. As a result, the dq-axis flux linkages λ_d and λ_q are generated on the dq-axis windings of the armature. If time constant of the field winding is large enough, the flux linkage with the field winding λ_{fd} is kept constant and held to maximum of $M_{fd}i_d$.

$$\left. \begin{aligned} \lambda_d &= L_d i_d + M_{fd} i_{fd} \\ \lambda_q &= L_q i_q \\ \lambda_{fd} &= M_{fd} i_d + L_{fd} i_{fd} \end{aligned} \right\} \quad (3)$$

where L_d, L_q : dq-axis self inductance, L_{fd} : field winding self inductance, M_{fd} : mutual inductance.

As the direct current i_q is produced on the q-axis winding which moves synchronously with the mover, thrust F is obtained from the following equation.

$$F = \frac{\pi}{\tau} (\lambda_d i_q - \lambda_q i_d) \quad (4)$$

Though a pulsating component exists in the thrust, practically it is not serious problem by choosing the bias frequency suitably.

III. CHARACTERISTICS OF THE NOVEL LSM

A. Analytical Model

Fig. 3(a) shows an analytical model of the proposed traction system using the short-armature type novel LSM with short pitch armature windings and Fig. 3(b) shows the overall view. The design parameters are shown in Table I that are decided on the basis of our long-armature type experimental equipment [1]. Three phase currents of (1) are supplied to the stator armature coils. For the grounded field coils the power supply is not necessary.

B. Analytical Result

The performance characteristics are investigated by an electric and magnetic coupled analysis using the FEM software.

Fig. 4 shows the flux distributions. It is confirmed that the

field fluxes are produced by the armature currents. However, end effect is detected on both sides of the mover slots where traveling fluxes don't exist and under where field fluxes are rarely produced. The induced field current and thrust are shown in Fig. 7 and Fig. 8.

TABLE I DESIGN PARAMETERS OF THE ANALYTICAL MODEL

Field	Number of Poles	16
	Windings	500 turns / pole
Armature	Number of Poles	4
	Windings	Double Layer Short Pitch Factor 2/3 85 turns / phase
	Resistance	1.24 Ω
Pole Pitch		60 mm
Air Gap		0.6 mm
Stack Height		50 mm

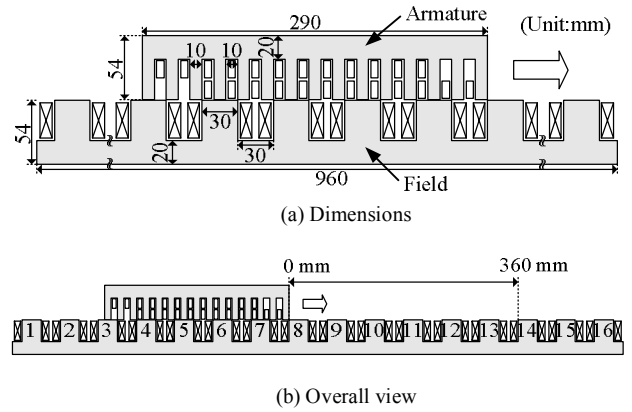


Fig. 3. Analytical model of the short pitch winding type system.

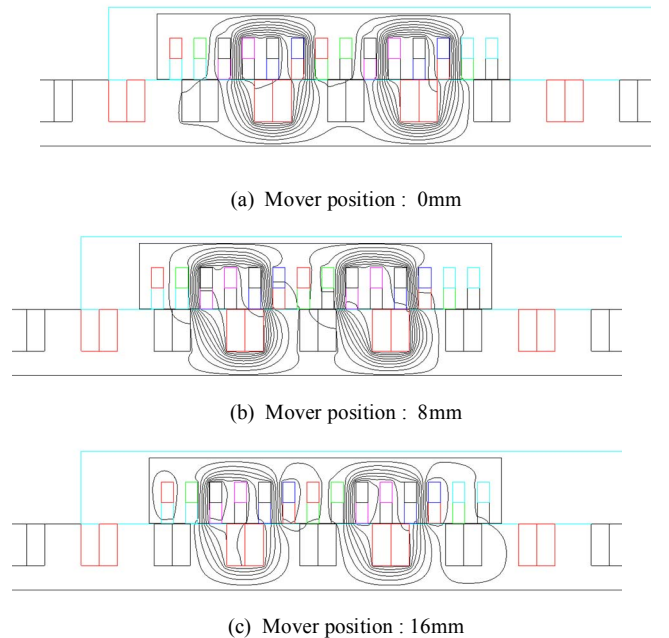


Fig. 4. Flux distributions of the usual short pitch winding type

IV. COMPENSATED ARMATURE WINDINGS

A. Performance Characteristics

Though the end effect is reduced by increasing the number of stator poles and increasing the stator length, that is constrained by boggy length of the transport system. Fig. 5 shows the new type mover with compensated armature windings in order to expand the traveling flux region and decrease the end effect. Fig. 6 shows the flux distributions. It is shown that the number of poles of the traveling flux increase from 4 to 6 as compared with Fig. 4.

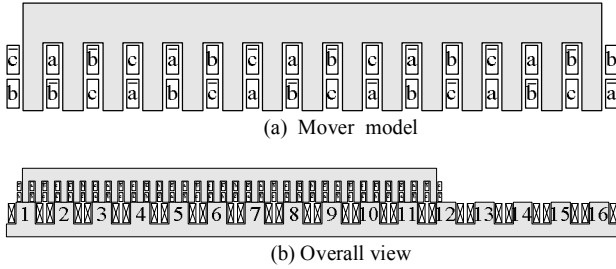


Fig. 5. Mover model with compensated armature windings.

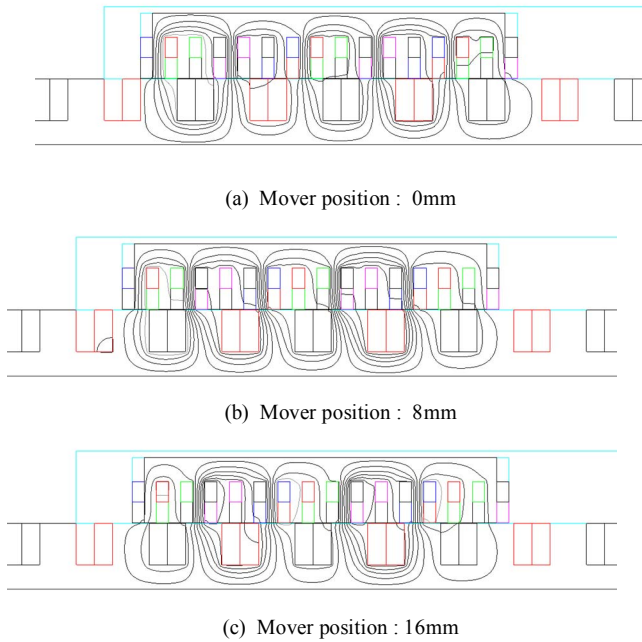


Fig. 6. Flux distributions of the compensated armature winding type

Fig. 7 compares the induced field current of the usual short pitch winding type and compensated short pitch winding type. Field current of the compensated short pitch winding type is increased in distance of longitudinal direction (from 260 mm to 330 mm) and the maximum value (from 0.68 A to 0.83 A). Therefore both maximum and average torque of the compensated winding type increase rather than the usual short pitch winding type, as shown in Fig. 8. When effective value of the excitation current command is 1 A and that of the thrust current command is 1 A, the average thrust of the compensated winding type is larger than the usual short pitch winding type

by 28%, as shown in Table II.

B. Effect of Field Structure

Fig. 9(a), (b) show the thrust-position characteristics where the field coils are connected in series over 1 pole, 2 poles, 3 poles and 4 poles. Fig. 10 shows the average thrust of them. It is shown that the average thrusts are almost constant without according to the series connected number of poles.

Fig. 11(a) shows the analytical model when the field iron cores are separated but located closely (the distance equals to 0.01 mm) and Fig. 11(b) shows when they are separated each other (the distance equals to 30 mm). The number of series-connected field poles are 2 so that the field windings of pole 1 and 2 of the Fig. 5(b), for examples, are series-connected with a diode. Fig. 12 shows their thrusts comparing with no-separated field core (the distance is 0). The average thrust of the separated field iron core type decreases by 20% in comparison with the no-separated type. But the thrust of the closely located type is same as the no-separated type.

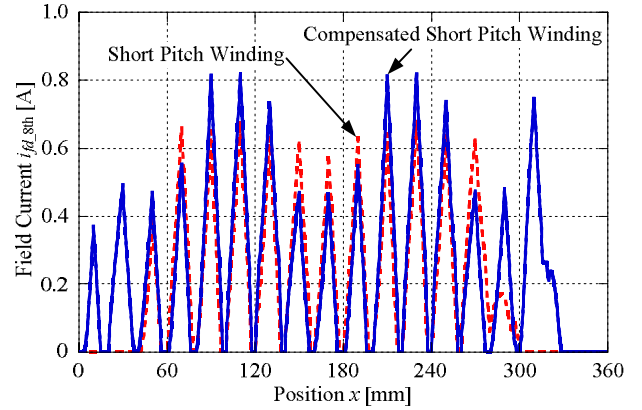


Fig. 7. Field current-position characteristic. (8th field pole)

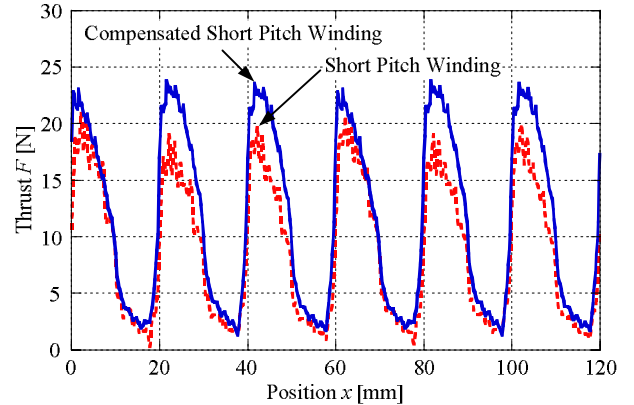
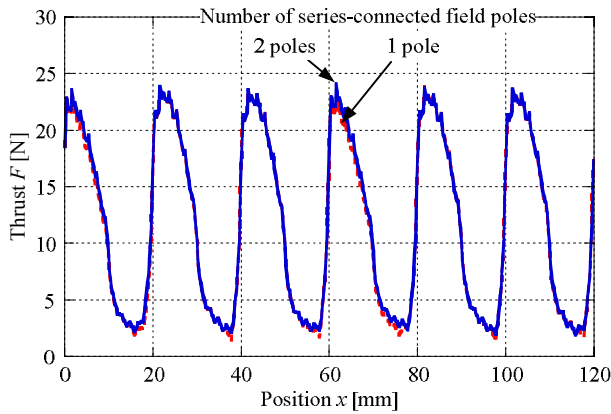


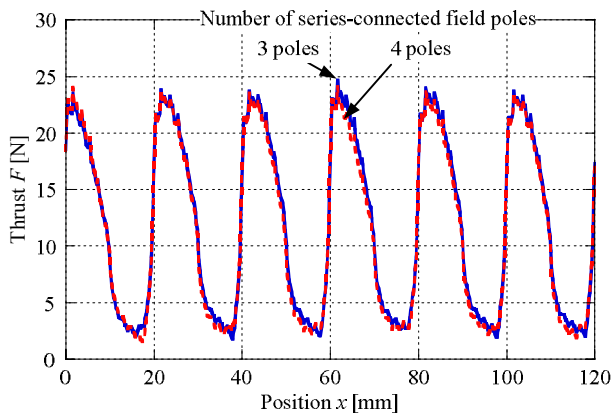
Fig. 8. Thrust-position characteristic.

TABLE II AVERAGE THRUST

	Average Thrust F_{avg} [N]
Short Pitch Winding	9.03
Compensated Short Pitch Winding	11.55



(a) Number of series-connected field poles : 1 pole, 2 poles



(b) Number of series-connected field poles : 3 poles, 4 poles

Fig. 9. Thrust-position characteristic.

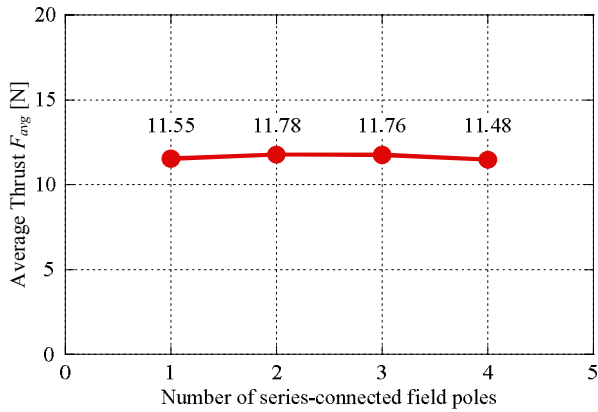


Fig. 10 Average thrust

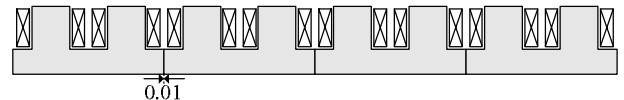
V. CONCLUSIONS

The short-armature self-excitation type novel LSM applicable for a transport system was proposed and the performance characteristics were computed using the electric and magnetic coupled analysis.

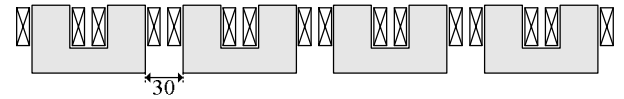
It was confirmed that the compensated short pitch windings are effective at reducing the end effect.

REFERENCES

- [1] J. Oyama, T. Higuchi, T. Abe, S. Kubota and T. Hirayama, "Principle and Analysis of a Novel Linear Synchronous Motor with Half-Wave Rectified Self Excitation", Proc. of the 17th International Conference on Magnetically Levitated Systems and Linear Drives, No.PP07109, pp.1-6(2002.9)
- [2] T. Hirayama, J. Oyama, T. Higuchi, T. Abe, "Modeling of a Linear Synchronous Motor with Half-Wave Rectified Self Excitation using Circuit Simulator", Proc. of the Fifth International Symposium on Linear Drives for Industry Applications, pp.532-535, (2005.9)
- [3] J. Oyama, T. Higuchi, T. Abe, T. Hirayama, T. Yoshida, "Characteristic Analysis for Short-Stator Type Linear Synchronous Motor with Half-Wave Rectified Self Excitation", Proc. of International Conference on Electrical Machines and Systems, No.DS1E2-08, pp.1-4(CD-ROM)(2006)



(a) Closely located (Distance : 0.01mm)



(b) Separated (Distance : 30mm)

Fig. 11. Location of field iron cores

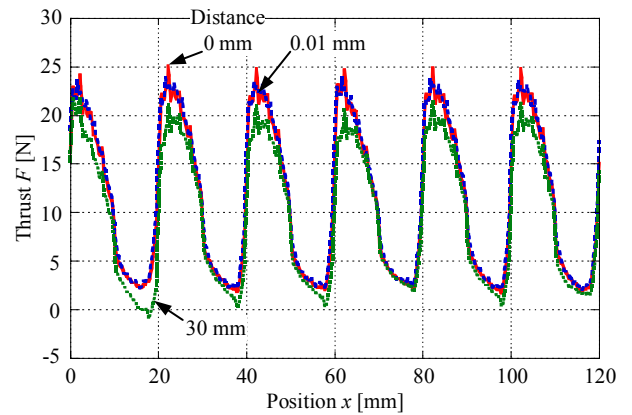


Fig. 12. Thrust-position characteristics.
(Number of series-connected field poles : 2 poles)

TABLE III AVERAGE THRUST

Distance	Average Thrust F_{avg} [N]
0 mm	11.75
0.01 mm	11.40
30 mm	9.66